Photomedicine and Laser Surgery
Volume 28, Supplement 2, 2010

Pp. S89–S97
DOI: 10.1089/pho.2009.2674

Raman Spectroscopy Validation of DIAGNOdent-Assisted Fluorescence Readings on Tibial Fractures Treated with Laser Phototherapy, BMPs, Guided Bone Regeneration, and Miniplates

Antonio L.B. Pinheiro, Ph.D.,[1,2,3] Cibelle B. Lopes, Ph.D.,[4] Marcos T.T. Pacheco, Ph.D.,[2] Aldo Brugnera, Junior, Ph.D.,[2] Fátima Antonia A. Zanin, Ph.D.,[5] Maria Cristina T. Cangussú, Ph.D.,[6] and Landulfo Silveira, Junior, Ph.D.[2]

Abstract

Objectives: We aimed to assess through Raman spectroscopy and fluorescence the levels of calcium hydroxyapatite (CHA) and lipids and proteins in complete fractures treated with internal rigid fixation (IRF) treated or not with laser phototherapy (LPT) and associated or not with bone morphogenetic proteins (BMPs) and guided bone regeneration (GBR). ***Background:*** Fractures have different etiologies and treatments and may be associated with bone losses. LPT has been shown to improve bone healing. ***Methods:*** Tibial fractures were created on 15 animals and divided into five groups. LPT started immediately after surgery, repeated at 48-h intervals. Animal death occurred after 30 days. ***Results:*** Raman spectroscopy and fluorescence were performed at the surface. Fluorescence data of group IRF + LPT + Biomaterial showed similar readings to those of the group IRF-no bone loss. Significant differences were seen between groups IRF + LPT + Biomaterial and IRF + LPT; IRF + LPT + Biomaterial; and IRF + Biomaterial; and between IRF + LPT + Biomaterial and IRF. CH groups of lipids and proteins readings showed decreased levels of organic components in subjects treated with the association of LPT, biomaterial, and GBR. Pearson correlation showed that fluorescence readings of both CHA and CH groups of lipids and proteins correlated negatively with the Raman data. ***Conclusions:*** The use of both methods indicates that the use of the biomaterials associated with infrared LPT resulted in a more-advanced and higher quality of bone repair in fractures treated with miniplates and that the DIAGNOdent may be used to perform optical biopsy on bone.

Introduction

We have used Raman spectroscopy as a method of assessment of the effects of laser phototherapy (LPT) on bone healing by using different models,[1–5] including in fractures.[6] Our previous results indicate that near-infrared (NIR) laser phototherapy (LPT) is effective to improve bone repair, mainly because of its greater penetration on bone when compared with visible laser light.[7–16] The use of LPT in studies involving bone healing is a hot topic, and many have demonstrated positive results, even when associated with biomaterials.[1–6,9,11–15]

Our experience indicates that LPT is more effective if used at early stages of healing. It is known that the positive stimulatory effect of laser light on bone occurs during the initial phase of proliferation of both fibroblasts and osteoblasts, as well as on initial differentiation of mesenchymal cells. Both fibroblastic proliferation and secretion are increased in irradiated subjects and in cell cultures. In bone, undifferentiated mesenchymal cells change to a fibroblast-like cells that later become osteoblasts, responsible for a marked amount of collagen fibers on irradiated bone.[9]

We have proven that improvement in bone maturation in irradiated subjects is associated with the increased deposition

[1]Center of Biophotonics, School of Dentistry, Federal University of Bahia, Salvador, BA, Brazil.
[2]Universidade Camilo Castelo Branco, São José dos Campos, SP, Brazil.
[3]Instituto Nacional de Ciência e Tecnologia de Óptica e Fotônica, São Carlos, SP, Brazil.
[4]Dental School, FCS, UNIVAP, S. J. Campos, SP, Brazil.
[5]Instituto Brugnera & Zanin, São Paulo, SP, Brazil.
[6]Dental Public Health, School of Dentistry, Federal University of Bahia, Salvador, Brazil. BA.

of calcium hydroxyapatite (CHA) during the early stages of healing. This maturation probably represents the increased capacity of secretion by the osteoblasts in irradiated subjects. It is well accepted that deposition of CHA represents bone maturation with the larger amounts of CHA in bone being indicative of more-resistant and calcified bone.[6,7,10] It is known that LPT has the ability to stimulate cell proliferation, including that of osteoblasts, and these cells have the capacity to secrete collagen, a main organic component observed during bone repair.[1–5,8,11–14]

The effect of LPT on bone tissue is not much evident before 30 days after treatment.[1–5,8,11–14] This may be because, during early stages of bone healing, the cellular component is more prominent and more prone to be affected by the laser light. Later, the bone matrix will be the main component of the healing bone. Our experience indicates that the application of LPT at early stages is more effective when the cellular component is greater. Later, the increased number of cells leads to greater deposition of bone matrix that later incorporates CHA, characterizing maturation of the bone.[1–5,8,11–14]

Many techniques are used to improve bone healing. Recently, LPT has been used for improving bone healing in several conditions, such as in dental implants[7,10,15] and autologous bone grafts,[4,8] and in several types of bone defects.[1–5] Several studies demonstrated that NIR LPT is the most suitable for bone repair because of its greater penetration depth in bone tissue compared with visible laser light.[9] Although the use of LPT on the bone healing has been increasing steadily, and several studies have demonstrated positive results in the healing of bone tissue, few reports exist on the association of LPT and biomaterials.[1–4,6,9,11–14]

The healing of a fracture is a complex and interesting process. In optimal conditions, injured bone can be reconstituted without a scar, almost identical to its original shape. The treatment of fractures consists of the reduction and fixation of dislocated segments. Open reduction and internal fixation of fractures is used to restore bone anatomy and to allow early mobilization. These procedures also overcame the limitations encountered when fractures are treated with skeletal traction or cast immobilization. The use of internal fixation in the treatment of fractures provides sufficient stability for fracture healing without excessive rigidity. The choice of the method of internal fixation depends on the type of fracture; on the condition of the soft tissues and bone; on the size and position of the bone fragments; and on the size of the bony defect. The main goal of internal fixation is the achievement of prompt and, if possible, full function of the injured bone, with rapid rehabilitation of the patient. The majority of internal-fixation devices are currently made of stainless steel. Numerous devices are available for internal fixation. These devices can be roughly divided into a few major categories: wires; pins and screws; plates; and intramedullary nails or rods.[6]

Traditional plate-and-screw constructs follow the tenets that include direct fracture exposure with anatomic reduction of fracture fragments and rigid internal fixation. The desired result of this intervention is anatomic bone union. Complications with these techniques include delayed union, nonunion; refracture after device removal; and infection.[6]

Metal plates for internal fixation of fractures have been used for more than 100 years. Improvements in the metallurgic formulation increased corrosion resistance. Although initial shortcomings, such as corrosion and insufficient strength, have been overcome, more-recent designs have not solved all problems.[6] The majority of plates are made of stainless steel or titanium. With flexible fixation, the fracture fragments displace in relation to each other when a load is applied across the fracture site. Fracture fixation is considered flexible if it allows appreciable interfragmentary movement under functional loads. The function of standard plate-and-screw constructs depends on the stability requirements of a particular fracture.[6]

In some fractures, handling is further complicated by the loss of bone that may be related to several etiologies and may require further efforts from the body to recover fully. Among the options available to minimize bone loss is the use of grafts. Although grafts have been used to minimize the problems associated with bone loss, considerable limitations associated with the use of autografts and allografts have prompted an increased interest in the use of bone-graft substitutes.[9]

Raman scattering is a powerful light-scattering technique used to analyze the internal structure of molecules. Raman spectroscopy is based on the measurement of both wavelength and intensity of inelastically scattered light. Raman scattered light occurs at wavelengths that are shifted from the incident light by the energies of the molecular vibrations. Although the mechanism of Raman scattering is different from that of infrared absorption, it provides complementary information. Its applications include structure determination and multicomponent qualitative and quantitative analysis.[6,7,10]

The Raman spectrum of bone shows prominent vibrational bands related to tissue composition. Some main Raman bands on tissues are at 862, 958, 1,070, 1,270, 1,326, 1,447, and 1,668 cm^{-1}. The 1,668 cm^{-1} band and those at 1,270 and 1,326 cm^{-1} are attributed to amide I and amide III stretching modes; the ones at 958 and 1,070 cm^{-1} are attributed to phosphate and carbonate hydroxyapatite, respectively. The band at 862 cm^{-1} can be attributed to the vibration bands of C–C and C–C–H stretches of collagen and lipid. The band at 1,447 cm^{-1} is attributed to the bending and stretching modes of CH groups of lipids and proteins.[6]

This technique has been used by our team in several noninvasive diagnostic applications of biologic samples, such as around dental implants; bone healing; and in association with biomaterials.[6,7,10] Our results indicate that it is a viable tool for the study of both mineralization and organic components of the healing bone. This technique has been shown to be a gold standard for the assessment of bone healing by our group.[6,7,10]

Some molecules are able to interact with light; the absorption of the light occurs on the chromophores. In molecules capable of absorbing and emitting light by fluorescence, the absorbing sites are known as fluorophores. These are functional groups in a molecule that will absorb energy of a specific wavelength and re-emit energy at a different (but equally specific) wavelength. The amount and wavelength of the emitted energy will depend on both the fluorophore and its chemical environment. In this group, we include flavins, proteins, collagen, elastin, NADH, and porphyrins.[1]

The intensity of the fluorescence is directly related to the amounts of fluorophores. Although most of the fluorescence found in living organisms is related to organic components,

apatite also plays a small role.[17,18] Different levels of fluorescence may result from the combination of both organic and inorganic components.[19,20] The fluorescence of several structures has been determined by the awareness of both absorption and emission spectra of the fluorophores present in biologic tissues.[21]

It has been shown that dental calculus, dental plaque, dental sealers, stains, restorative materials, and remnants of toothpaste may also produce fluorescence and lead to false-positive readings.[22–25] It has been found that the high level of fluorescence of the dental calculus is due to the presence of bacteria.[26]

The DIAGNOdent contains a laser diode (λ655 nm) as the excitation light source and a photo diode combined with a long-pass filter (transmission, $>\lambda$680 nm) as the detector. The excitation light is transmitted by an optical fiber to the tooth, and a bundle of nine fibers arranged concentrically around it serves for detection. The long-pass filter absorbs the back-scattered excitation and other short-wavelength light and transmits the longer-wavelength fluorescence radiation. To eliminate the long-wavelength ambient light also passing through the filter, the laser diode is modulated, and only light showing the same modulation characteristic is registered. Thus, the digital display shows quantitatively the detected fluorescence intensity.

The initial studies with this equipment found that, in addition to a small amount of water and organic matrix, enamel contains modified hydroxyapatite, a carbonate-substituted calcium-deficient apatite. A small baseline fluorescence level was observed for sound enamel and a different fluorescence level after the caries process has started. To test the contributions of various calcium phosphates (*e.g.*, tricalcium phosphate, dicalcium phosphate-dihydrate, calcium carbonate) to the fluorescence signal, we measured fluorescence of pure pellets with excitation at λ655 nm.[27]

The relative fluorescence signals of these pellets were between 3% and 12%, compared with that of human enamel.[19] It has been found that it is unlikely the calcium phosphates are responsible for the baseline fluorescence of sound teeth. Baseline fluorescence might be the result of combining the inorganic matrix with absorbing organic molecules.[28] It also was found that the fluorescence of whiter teeth is less compared with that of darker teeth. Presumably, the same stains affect tooth color and baseline fluorescence. Furthermore, it is important to note that calculus, plaque hypomineralization, composite filling materials, remnants of polishing pastes, and stains may produce fluorescence.[18,23–25,29] Therefore, they may cause false-positive readings when the DIAGNOdent is calibrated with respect to sound enamel.[27] Several studies included its use on occlusal and smooth surfaces[18,20,23,30–32] and compared it with visual inspection, histology, radiography, and quantitative light-induced fluorescence. Good intraexaminer reproducibility on occlusal and accessible smooth surfaces was reported *in vivo* under daily practice conditions[23,25,33] and *in vitro*.[18,24,32,34] The only investigation that assessed interexaminer reproducibility on smooth surfaces showed a substantial κ value of 0.77.[33] Our group also worked previously with this device.[35–37]

The aim of this study was to evaluate and validate the use of the DIAGNOdent as a method of optical biopsy, through the analysis of Raman spectra intensity, the incorporation of CHA (958 cm^{-1}; phosphate) and organic components (CH groups of lipids and proteins, 1,447 cm^{-1}) on the repair of complete tibial fracture in rabbits treated with IRF (miniplates) associated or not with the use of laser therapy (λ790 nm) or the use of BMPs and guided bone regeneration, or both.

Material and Methods

This study was approved by the Animal Ethics Committee of the Universidade do Vale do Paraíba. Fifteen healthy adult male New Zealand rabbits (average weight, 2 kg) were kept under natural conditions of light, humidity, and temperature at the Animal House of the Instituto de Pesquisa e Desenvolvimento da Universidade do Vale do Paraíba during the experimental period. The animals were fed with standard laboratory pelleted diet and had water *ad libidum*. The animals were kept in individual metallic cages with a day/night light cycle and controlled temperature during the experimental period.

Under general anesthesia (0.2% Acepran, 1 mg/kg,[1] and Zoletil, 50 mg, 15 mg/kg,[2] the animals had the right leg shaved, and a 4-cm-long incision was performed at the right tibia with a number 15 scalpel blade. Skin and subcutaneous tissues were dissected down to the periosteum, which was gently sectioned, exposing the bone. One tibial complete bone fracture was surgically produced in each animal by using a low-speed drill (1,200 rpm) under refrigeration. This model was used previously by our team.[6] A 5-mm piece of bone was removed in all animals, except in one group (IRF_NBL). The random distribution of the animals in each group of five can be seen in Table 1.

All groups had open fracture reduction and fixation with miniplates (titanium). In the group IRF + Bone Loss, the fragments were fixed with the miniplates, leaving a 5-mm gap. In groups IRF + Bone Loss + Biomaterial + GBR and IRF + Bone Loss + Biomaterial + GBR + LPT, the defect was filled with lyophilized organic bovine bone (Gen-ox-org),[3] collagen (Gen-col),[3] bone morphogenetic proteins (Gen-pro),[3] and covered with decalcified cortical osseous membrane (Gen-derm).[3] In groups IRF + Bone Loss + LPT and IRF + Bone Loss + Biomaterial + GBR + LPT (Diode Laser

Table 1. Distribution of Each Animal on the Experimental Groups

Group	*Treatment*	*Bone Loss*	*Biomaterial + Guided Bone Regeneration*	*LPT*
I	IRF	Yes	No	No
II	IRF	Yes	Yes	No
III	IRF	Yes	No	Yes
IV	IRF	Yes	Yes	Yes
V	IRF_NBL	No	No	No
VI	Bone	No	No	No

IRF, internal rigid fixation; IRF_NBL, internal rigid fixation no bone loss.

[1]Univet S.A, São Paulo, SP, Brazil, Butorfanol® 0.02 ml/kg, Fort Dodge, Campinas, SP, Brazil.
[2]VIRBAC S.A, Carro Cedex, France.
[3]Baumer S/A, Mogi Mirim, SP, Brazil 3.

Unit; Kondortech, São Carlos, SP, Brazil; λ790 nm, 40 mW, $\varphi \sim 0.5\,cm^2$) was transcutaneously applied in four points around the defects at 48-h intervals ($4\,J/cm^2$, per point). The first session was carried out immediately after surgery and repeated every 48 h for 15 days ($16\,J/cm^2$ per session) and a total treatment dose of $112\,J/cm^2$. To standardize the location of irradiation, four tattoos were made on the skin by using China Ink around the fracture immediately after surgery to allow irradiation to be carried out at the same point. Doses used here are based on previous studies carried out by our group.[1–6] In group IRF_NBL, the fracture had no bone loss and was manually reduced and fixed with the miniplates. Normal bone acted as the control (Bone).

All wounds were routinely sutured, and the animals received a single dose of pentabiotico,[4] immediately after surgery. The animals were humanely killed 30 days after the surgery with an overdose of general anesthetics.

The samples were longitudinally cut under refrigeration,[5] and the specimens were stored in liquid nitrogen to minimize the growth of aerobic bacteria[38–40] and because chemical fixation is not advisable because of fluorescence emissions from the fixative substances.[38–40]

Before Raman study, the samples were longitudinally cut and warmed gradually to room temperature, and 100 ml of saline was added to the surface during spectroscopic measurements. For Raman measurements, a $\lambda = 830$ nm Ti: sapphire laser[6] pumped by argon laser[7] provided near-infrared excitation. A spectrograph[8] with a spectral resolution of about 8 per centimeter dispersed the Raman-scattered light from the sample, and a liquid nitrogen–cooled deep depletion CCD[9] detected the Raman spectra. The system was controlled by a microcomputer, which stored and processed the data.[6,7,10] The laser power used on the sample was 80 mW, with spectral acquisition time of 100 sec. Four points measured in the transverse cut of the bone healing resulted in four readings of each specimen and 52 total spectra. All spectra were collected on the same day to avoid optical misalignments and changes in laser power. The mean value of the intensity of the peaks ($958\,cm^{-1}$, phosphate ν_1 and at $1{,}447\,cm^{-1}$, CH groups of lipids and proteins ν_1) were determined by the average of the peaks in this region. This intensity is related to the concentration of CHA and organic components in the bone. The data were analyzed with the MatLab5.1 software[10] for calibration and background subtraction of the spectra. For calibration, the Raman spectrum of a solvent indene with known peaks was used[38–40] because of its intense bands in the region (800–$1{,}800\,cm^{-1}$) of our interest. We also measured the indene spectrum each time the sample was changed to be sure that the laser and collection optics were optimized. To remove the "fluorescence background" from the original spectrum, a fifth-order polynomial fitting was found to give better results, facilitating the visualization of the peaks of CHA ($\sim 958\,cm^{-1}$) and of CH groups of lipids and proteins ($1{,}447\,cm^{-1}$) found on the bone (Fig. 1). This routine can also remove any continuum of offset background noise due to CCD readout and cooling. Statistical analysis was performed by using Minitab 12.0 software.[11] A baseline Raman spectrum of nontreated bone was produced and acted as the control.

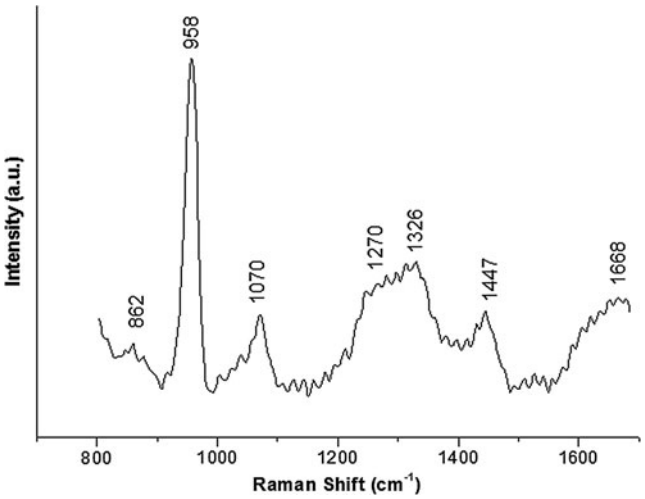

FIG. 1. Typical Raman spectra of bone components showing the two Raman shifts used as markers in the study ($\sim 958\,cm^{-1}$, CHA, and $1{,}447\,cm^{-1}$, CH groups of lipids and proteins.

The collection of the fluorescence (λ665 nm) readings was performed by a commercial device according to the instructions of the manufacturers (DIAGNODent2095, Kavo, Germany). Before the analysis of the specimens, a pilot study determined the mean values of the readings at the surface (baseline) of nontreated subjects. These data were statistically analyzed, and no significant differences were found between the readings of the tested samples ($p > 0.001$). In the experimental specimens, the data were collected twice: before the experiment (Baseline, 4 points at the surface) and at the end of the experimental time before the removal of the specimen (4 points at the fracture surface). The results were analyzed by using statistical software (Minitab 12.0; Belo Horizonte, MG, Brazil). Data normality was assessed with the Kolgomorov-Smirnof test. ANOVA and Tukey tests were used to identify differences between specific groups. Correlation between Raman and fluorescence data was carried out with Pearson correlation. The significance level in all cases was set at 5%.

Results

Laser fluorescence

A summary of the results of the fluorescence reading may be seen in Table 2. The results of the statistical analysis showed that the fluorescence readings of Group IRF + L + B showed similar readings to those of the group IRF_NBL. ANOVA showed significant differences between treatment groups ($p < 0.01$). The Tukey test showed significant differences

[4]Penicillin, streptomycin, 20.000 IU, Fort Dodge, Campinas, SP, Brazil.
[5]Bueler, Isomet TM1000; Markham, Ontario, Canada.
[6]Spectra Physics, model 3900S, Mountain View, CA.
[7]Spectra Physics, model 2017S, Mountain View, CA.
[8]Bruker Optics, model: 250 IS; Billerica, MA.
[9]Princeton Instruments, model LN/CCD-1024-EHR1; Tucson, AZ.
[10]Newark, NJ.
[11]Minitab, Belo Horizonte, MG, Brazil.

Table 2. Summary of the Results of the Fluorescence Readings Raman Shifts of CHA ($\sim 958 cm^{-1}$) and CH Groups of Lipids and Proteins ($\sim 1{,}447 cm^{-1}$)

Groups	*Mean Fluorescence Reading (au) ± SD*	*Mean Raman shift ($\sim 958\,cm^{-1}$) of CHA (au) ± SD*	*Mean Raman shift ($\sim 1{,}447\,cm^{-1}$) CH groups of lipids and proteins (au) ± SD*
IRF	7,667 ± 0,780	7,438 ± 1,393	5,609 ± 693
IRF + Biomaterial	8,000 ± 0,953	8,132 ± 1,946	6,296 ± 586
IRF + LPT	7,167 ± 0,718	8,723 ± 1,946	5,677 ± 942
IRF + LPT + Biomaterial	6,417 ± 0,900	9,316 ± 711	6,073 ± 390
IRF_NBL	6,417 ± 0,900	7,255 ± 2,855	6,014 ± 1,806
Bone	5,833 ± 0,718	1,1974 ± 725	8,955 ± 362

IRF, internal rigid fixation; IRF_NBL, internal rigid fixation, no bone loss.

between groups IRF + LPT + Biomaterial and IRF + LPT ($p = 0.03$); IRF + LPT + Biomaterial and IRF + Biomaterial ($p < 0.01$), and between IRF + LPT + Biomaterial and IRF ($p < 0.001$) (Fig. 2).

Raman spectroscopy

The Raman spectrum of bone shows prominent vibrational bands related to tissue composition. Figure 1 shows the main tissue Raman bands at 862, 958, 1,070, 1,270, 1,326, 1,447 and 1,668 cm^{-1}. The 1,668 cm^{-1} band and those at 1,270 and 1,326 cm^{-1} are attributed to amide I and amide III stretching modes, the ones at 958 and 1,070 cm^{-1} are attributed to phosphate and carbonate hydroxyapatite, respectively. The band at 862 cm^{-1} can be attributed to the vibration bands of the C-C and C-C-H stretch of collagen and lipid. The band at 1,447 cm^{-1} is attributed to the bending and stretching modes of CH groups of lipids and proteins. Figure 3 shows the value of the mean intensity of each Raman shift of hydroxyapatite (CHA, 958 cm^{-1}) obtained from all readings of treated and untreated subjects. The intensity of the Raman shift is directly related to the concentration/incorporation of CHA by the bone, so higher intensity represents a higher concentration of CHA. The results for the organic components (CH groups of lipids and proteins, 1,447 cm^{-1}) may be seen in Fig. 4. Higher peaks indicate less mineral content, and higher readings denote increased organic components. The results of the mean readings and standard deviation can be seen in Table 2.

The data were analyzed with the Kolmogorov-Smirnov test (5%) and were found to be normally distributed ($p = 0.37$). The analysis of the results of the concentration of CHA showed significant differences between the experimental groups (IRF + Bone Loss and IRF_NBL, $p = 0.05$, ANOVA) and between the experimental groups and untreated bone (Bone, $p < 0.001$, ANOVA). A paired t test showed significant differences between the untreated bone and the experimental groups IRF + Bone Loss ($p < 0.001$); IRF + Bone Loss + Biomaterial + GBR ($p < 0.001$); IRF + Bone Loss + LPT ($p < 0.001$); IRF + Bone Loss + Biomaterial + GBR + LPT ($p < 0.001$); and IRF_NBL ($p < 0.001$). Significant differences were also observed between groups IRF_NBL and IRF + Bone Loss + LPT ($p = 0.03$); IRF_NBL and IRF + Bone Loss + Biomaterial + GBR + LPT ($p = 0.02$); IRF + Bone Loss and IRF + Bone Loss + LPT ($p = 0.04$); IRF + Bone Loss and IRF + Bone Loss + Biomaterial + GBR + LPT ($p = 0.002$); and between IRF + Bone Loss + Biomaterial + GBR and IRF + Bone Loss + Biomaterial + GBR + LPT ($p = 0.05$; Fig. 3).

In the CH groups of lipids and proteins, significant differences between the Basal bone group and all treatment

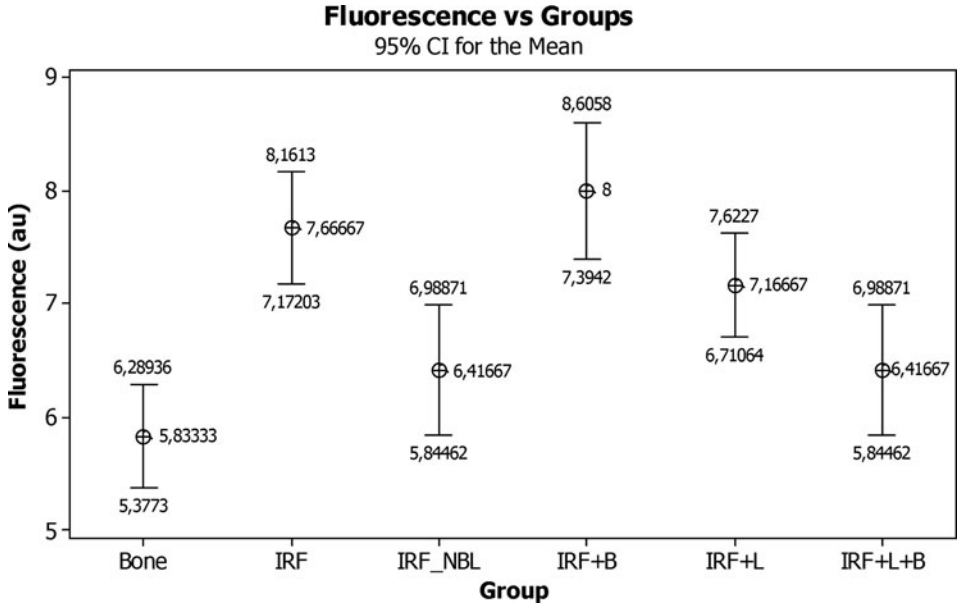

FIG. 2. Mean fluorescence readings and standard deviation of the experimental groups and basal bone. (IRF, internal rigid fixation; IRF_NBL, internal rigid fixation, no bone loss; B, biomaterial; L, LPT)

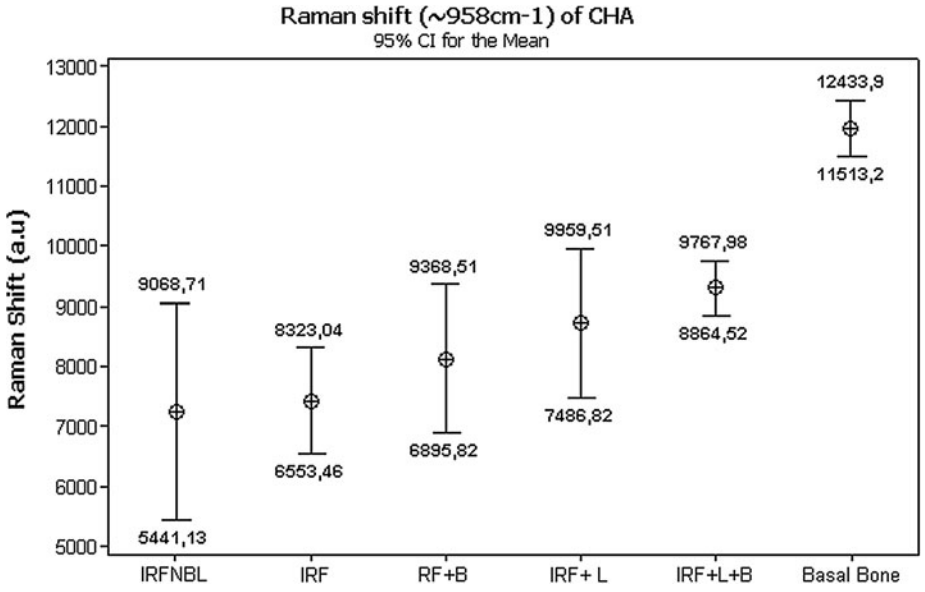

FIG. 3. Mean Raman intensity and standard deviation of hydroxyapatite (CHA, 958 cm^{-1}) obtained from all readings of treated and untreated subjects. (IRF, internal rigid fixation; IRF_NBL, internal rigid fixation, no bone loss; B, biomaterial; L, LPT)

groups was detected ($p < 0.001$) but not between treatments ($p = 0.4$). Paired t tests showed significant differences between Group Basal bone and all treatment groups ($p < 0.001$). Significant differences were also observed between groups IRF and IRF + GBR ($p = 0.005$) and between Groups IRF + GBR and IRF + LPT ($p = 0.03$; Fig. 4).

Pearson correlation between the fluorescence readings with the gold standard (CHA Raman Shift) was found to be negative and nonsignificant ($R^2 = -0.19$; $p = 0.12$). Despite not being significant statistically, these variables clearly show an inversely proportional relation, as seen in Fig. 5. When the CH groups of lipids and proteins Raman data were used, a significant negative correlation was observed ($R^2 = 0.22$; $p = 0.05$) (Fig. 6). This indicates an inversely proportional relation and that increased Raman peaks are positively related to higher fluorescence readings by the DIAGNOdent.

Discussion

LPT has been successfully used for improving bone healing in several conditions. The effects of LPT on bone are still controversial, as previous reports show different or conflicting results. It is possible that the effect of LPT on bone regeneration depends not only on the total dose of irradiation, but also on the irradiation time and the irradiation mode. Many studies indicated that irradiated bone, mostly with IR wavelengths, shows increased osteoblastic proliferation, collagen deposition, and bone neoformation when compared with nonirradiated bone. The irradiation protocol used in this study is similar to those used in previous reports. Our group has shown, by using different models, that association of bone grafts, bone morphogenetic proteins, and guided tissue regeneration does improve the healing of bone tissue.[1–16]

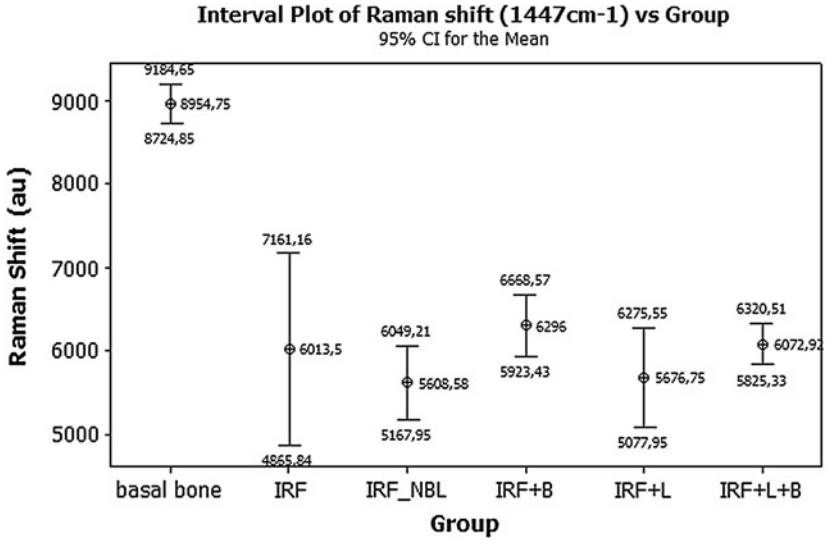

FIG. 4. Mean Raman intensity of each Raman shift of CH groups of lipids and proteins (1,447 cm^{-1}) obtained from all readings of treated and untreated subjects. (IRF, internal rigid fixation; IRF_NBL, internal rigid fixation, no bone loss; B, biomaterial; L, LPT)

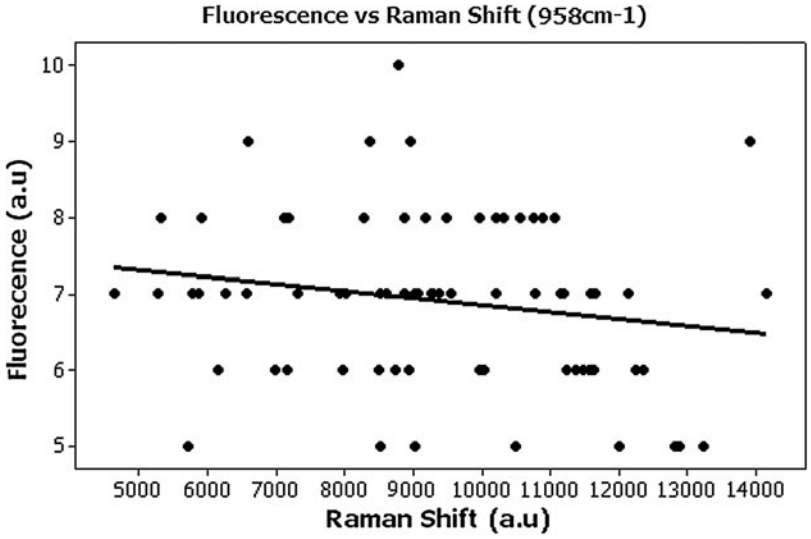

FIG. 5. Graphic of the Pearson correlation between the fluorescence readings with the gold standard CHA (958 cm^{-1}) Raman data.

Our team studied the effects of the use of LPT on bone by using several models, and we used different assessment methods to determine the effects of the laser on bone, including histology, computerized morphometry, SEM, and Raman spectroscopy. [1–16]

Raman spectroscopy was used to analyze both mineral and organic component changes on bone, and we considered it to be the gold standard for the study of bone components.[6,7,10]

One of the models we used is the bone fracture, a very complex model that allows several types of treatment, including the use of wire osteosynthesis[6] and miniplates. We also associated these methods with biomaterials and guided bone regeneration.[1–7,9–15] Our results were achieved with the use of protocols, models, and parameters previously reported by our team to be indicative that IR LPT is responsible for a quicker process as well as inproving the quality of the newly formed bone.[1–16]

Our experience indicates that the advanced maturation seen in irradiated bone is due to an increased deposition of CHA. The maturation represents the improved ability of the irradiated osteoblasts to secrete more CHA. Increased amounts of CHA are indicative of bone maturation as well as of a more resistant and calcified bone.[1–16]

The use of the DIAGNOdent is related mainly to the diagnosis of caries, and it has been shown to be effective in the detection of tricalcium phosphate, dicalcium phosphate-dihydrate, and calcium carbonate.[27] The fluorescence is affected by the color of the tooth, as same stains are able to alter the baseline fluorescence. Despite the lack of previous reports of the possibility of nanobacterias causing fluorescence, we consider their presence a potential factor causing fluorescence.[41] It has been shown that this equipment possesses good reproducibility both *in vivo*[23,25,33] and *in vitro*.[18,24,32,34]

We were unable to find any previous reports in the literature of the use of this device as an optical biopsy method, so we decided to validate this new application by using Raman spectroscopy as the gold standard.

We found that the fluorescence readings of Group IRF + LPT + Biomaterial showed similar readings to those of the group IRF_NBL and also found significant differences between treatment groups. Significant differences were seen

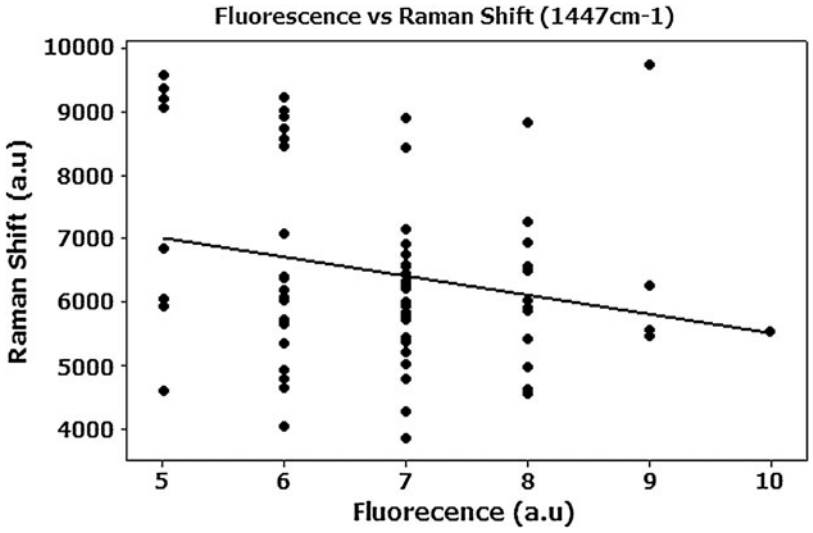

FIG. 6. The Pearson correlation between the fluorescence readings with the gold-standard CH groups of lipids and proteins (1,447 cm^{-1}) Raman data.

between groups IRF + LPT + Biomaterial and IRF + LPT; IRF + LPT + Biomaterial and IRF + Biomaterial and between IRF + LPT + Biomaterial and IRF.

Raman data of CHA readings indicates that the use of association of LPT, biomaterial, and GBR was efficacious in improving bone maturation and healing.[1–16] and that, in regard to the CH groups of lipids and proteins readings, the decrease in the level of organic components in subjects treated with the association of LPT, biomaterial, and GBR. Fewer organic components represent a more-mature bone.[1–16]

We used Pearson correlation to verify whether the fluorescence readings would correlate with the gold standard (Raman spectroscopy). We found that the fluorescence readings of both CHA and CH groups of lipids and proteins correlated negatively with the Raman data. These variables clearly show an inversely proportional relation and that increased Raman peaks are negatively related to higher fluorescence readings by the DIAGNOdent.

The use of both methods indicates that the use of the biomaterials associated with IR LPT resulted in a more-advanced and higher-quality bone repair in fractures treated with miniplates and that the DIAGNOdent may be used to perform optical biopsy on bone.

Author Disclosure Statement

No competing financial interests exist.

References

1. Pinheiro, A.L.B., Gerbi, M.M.E.M., Limeira Junior, F.A., et al. (2009). Bone repair following bone grafting hydroxyapatite guided bone regeneration and infra-red laser photobiomodulation: a histological study in a rodent model. Lasers Med. Sci. 24, 234–240.
2. Gerbi, M.M.E.M., Marques A.M.C., Ramalho, L.M.P., et al. (2008). Infrared laser light further improves bone healing when associated with bone morphogenic proteins: an in vivo study in a rodent model. Photomed. Laser Surg. 26, 55–60.
3. Pinheiro, A.L.B., Gerbi, M.M.E.M.A., Ponzi, E.A.C., et al. (2008). Infrared laser light further improves bone healing when associated with bone morphogenetic proteins and guided bone regeneration: an in vivo study in a rodent model. Photomed. Laser Surg. 26, 167–174.
4. Torres, C.S., Santos, J.N., Monteiro, J.S.C., et al. (2008). Does the use of laser photobiomodulation, bone morphogenetic proteins, and guided bone regeneration improve the outcome of autologous bone grafts? An in vivo study in a rodent model. Photomed. Laser Surg. 26, 371–377.
5. Gerbi, M.M.E.M., Pinheiro, A.L.B., Ramalho, L.M.P., et al. (2008). Effect of IR laser photobiomodulation on the repair of bone defects grafted with organic bovine bone. Lasers Med. Sci. 23, 313–317.
6. Lopes, C.B., Pacheco, M.T.T., Silveira Junior, L., et al. (2007). The effect of the association of NIR laser therapy BMPs, and guided bone regeneration on tibial fractures treated with wire osteosynthesis: Raman spectroscopy study. J. Photochem. Photobiol. B Biol. 89, 125–130.
7. Lopes, C.B., Pinheiro, A.L.B., Sathaiah, S., et al. (2007). Infrared laser photobiomodulation (830 nm) on bone tissue around dental implants: a Raman spectroscopy and scanning electronic microscopy study in rabbits. Photomed. Laser Surg. 25, 96–101.
8. Weber, J.B.B., Pinheiro, A.L.B., Oliveira, M.G., et al. (2006). Laser therapy improves healing of bone defects submitted to autogenous bone graft. Photomed. Laser Surg. 24, 38–44.
9. Pinheiro, A.L.B., and Gerbi, M.M.E.M. (2006). Photoengineering of bone repair processes. Photomed. Laser Surg. 24, 169–178.
10. Lopes, C.B., Pinheiro, A.L.B., Sathaiah, S., et al. (2005). Infrared laser light reduces loading time of dental implants: a Raman spectroscopy study. Photomed. Laser Surg. 23, 27–31.
11. Gerbi, M.M.E.M., Pinheiro, A.L.B., Ramalho, Marzola, C., et al. (2005). Assessment of bone repair associated with the use of organic bovine bone and membrane irradiated at 830 nm. Photomed. Laser Surg. 23, 382–388.
12. Gerbi, M.M.E.M., Pinheiro, A.L.B., Ramalho, Marzola, C., et al. (2005). Assessment of bone repair associated with the use of organic bovine bone and membrane irradiated at 830-nm. Photomed. Laser Surg. 23, 382–388.
13. Pinheiro, A.L.B., Limeira Júnior, F.A., and Gerbi, M.M.E.M., (2003). Effect of low level laser therapy on the repair of bone defects grafted with inorganic bovine bone. Braz. Dent. J. 14, 177–181.
14. Pinheiro, A.L.B., Limeira Júnior, F.A., Gerbi, M.M.E.M., et al. (2003). Effect of 830-nm laser light on the repair of bone defects grafted with inorganic bovine bone and decalcified cortical osseous membrane. J. Clin. Laser Med. Surg. 21, 383–388.
15. Pinheiro, A.L.B., Oliveira, M.A.M., and Martins, P.P.M. (2001). Biomodulação da cicatrização óssea pós-implantar com o uso da laserterapia não-cirúrgica: estudo por microscopia eletrônica de varredura. Rev. FOUFBA 22, 12–19.
16. Silva Junior, N., Pinheiro, A.L.B., Oliveira, M.G.A., et al. (2002). Computerized morphometric assessment of the effect of low-level laser therapy on bone repair: an experimental animal study. J. Clin. Laser Med. Surg. 20, 83–88.
17. Mendes, F.M., Pinheiro, S.L., and Bengtson, A.L. (2004). Effect of alteration in organic material of the occlusal caries on DIAGNOdent readings. Braz. Oral Res. 18, 141–144.
18. Tranaeus, X.Q., Shi, S., and Angmar-Mansson, B. (2001). Validation of DIAGNOdent for quantification of smooth-surface caries: an in vitro study. Acta Odont. Scand. 59, 74–58.
19. Hibst, R., Paulus, R., and Lussi, A. (2001). Detection of occlusal caries by laser fluorescence: basic and clinical investigations. Med. Laser Appl. 16, 205–213.
20. Hosoya, Y., Taguch, T., Arita F., and Tay, S. (2008). Clinical evaluation of polypropylene glycol-based caries detecting dyes for primary and permanent carious dentin. J. Dent. 36, 1041–1047.
21. Leblanc, L., and Dufour, E. (2002). Monitoring the identity of bacteria using their intrinsic fluorescence. FEMS Microbiol. Lett. 211, 147–153.
22. Lussi, A., and Reich, E. (2005). The influence of toothpastes and prophylaxis pastes on fluorescence measurements for caries detection in vitro. Eur. J. Oral Sci. 113, 141–144.
23. Lussi, A., Megert, B., Longbottom, C., et al. (2001). Clinical performance of a laser fluorescence device for detection of occlusal caries lesions. Eur. J. Oral Sci. 109, 14–19.
24. Lussi, A., Imwinkelried, S., Pitts, N.B., et al (1999). Performance and reproducibility of a laser fluorescence system for detection of occlusal caries in vitro. Caries Res. 33, 261–266.

25. Sheehy, E.C., Brailsford, S.R., Kidd, E.A., et al. (2001). Comparison between visual examination and a laser fluorescence system for in vivo diagnosis of occlusal caries. Caries Res. 35, 421–426.
26. Sailer, R., Paulus, R., and Hibst, R. (2001). Analysis of carious lesions and subgingival calculi by fluorescence spectroscopy. Caries Res. 35, 267.
27. Lussi, A., Hibst, R., and Paulus, R. (2004). DIAGNOdent: an optical method for caries detection. J. Dent. Res. 83 Spec No C, C80–C83.
28. Hibst, R., and Paulus, R. (1999). Caries detection by red excited fluorescence: investigations on fluorophores. *Caries Res* 33, 295.
29. Farah, R.A., Drummond, B.K., Swain, M.V., et al. (2008). Relationship between laser fluorescence and enamel hypomineralisation. J. Dent. 36, 915.
30. Anttonnen, V.L., Seppä, L., and Hausen, H. (2003). Clinical study of the use of the laser fluorescence device DIAGNOdent for detection of occlusal caries in children. *Caries Res.* 37, 17–23.
31. Côrtes, D.F., Ellwood, R.P., and Ekstrand, K.R. (2003). An in vitro comparison of a combined FOTI/visual examination of occlusal caries with other caries diagnostic methods and the effect of stain on their diagnostic performance. *Caries Res* 37, 8–16.
32. Lussi, A., and Francescut, P. (2003). Performance of conventional and new methods for the detection of occlusal caries in deciduous teeth. *Caries Res* 37, 2–7.
33. Pinelli, C., Campos Serra, M., and De Castro Monteiro, l.l. (2002). Validity and reproducibility of a laser fluorescence system for detecting the activity of white-spot lesions on free smooth surfaces in vivo. *Caries Res* 36, 19–24.
34. Braga, M., Nicolau, J., Rodrigues, C.R., et al. (2008). Laser fluorescence device does not perform well in detection of early caries lesions in primary teeth: an in vitro study. Oral Health Prev. Dent. 6, 165–169.
35. Zanin, F., and Brugnera Junior., F. (2006). Diode laser in the diagnosis of carious lesion. In: *Atlas of Laser Therapy Applied to Clinical Dentistry*, Junior Brugnera, et al. (eds.). Germany: Quintessence Edit, pp. 91–97.
36. Zanin, F., Campos, D.H.S., Zanin, S., et al. (2001). Measurements of the fluorescence of restorative dental materials using a diode laser 655 nm. Laser Dent. 4249, 145–151.
37. Zanin, F., Brugnera Junior, A., Pinheiro, A.L.B., et al. (2001). Diagnóstico da lesão de cárie com a técnica a laser diodo 655nm. JADA 4, 245–249.
38. Silveira-Júnior, L., Sathaiah, S., Zângaro, R.A., et al. (2003). Near infrared Raman spectroscopy of human coronary arteries: histopathological classification based on Mahalanobis distance, J. Clin. Laser Med. Surg. 21, 203–208.
39. Nogueira, G.V., Silveira Júnior, L., Martin, A.A., et al. (2005). Raman spectroscopy study of atherosclerosis in human carotid artery, J. Biomed. Opt. 10, 031117-1–031117-7.
40. Morris, M.D., Stewart, S., Tarnowski, C.P., et al. (2002). Early mineralization of normal and pathologic calvaria as revealed by Raman spectroscopy, SPIE Proc. 4614, 28–39.
41. Zhang, S.M., Tian, F., Jiang, X.Q., Li, J., Xu C., Guo, X.K., and Zhang, F.Q. (2009). Evidence for calcifying nanoparticles in gingival crevicular fluid and dental calculus in periodontitis. J. Periodontol. 80, 1462–1470.

Address correspondence to:
Prof. Antonio L.B. Pinheiro
Center of Biophotonics
School of Dentistry
Federal University of Bahia
62 Araujo Pinho Ave, Canela
Salvador, BA
Brazil 40110-150

E-mail: albp@ufba.br